Schweizerische Eidgenossenschaft
Confédération suisse
Confederazione Svizzera
Confederaziun svizra

Federal Department of the Environment,
Transport, Energy and Communications DETEC

Swiss Federal Office of Energy
Energy Research and Cleantech

Interim report from 13 November 2024

earlyWARN

A Data-Driven Real-Time Dynamic Security Assessor and Early Warning System for TSOs

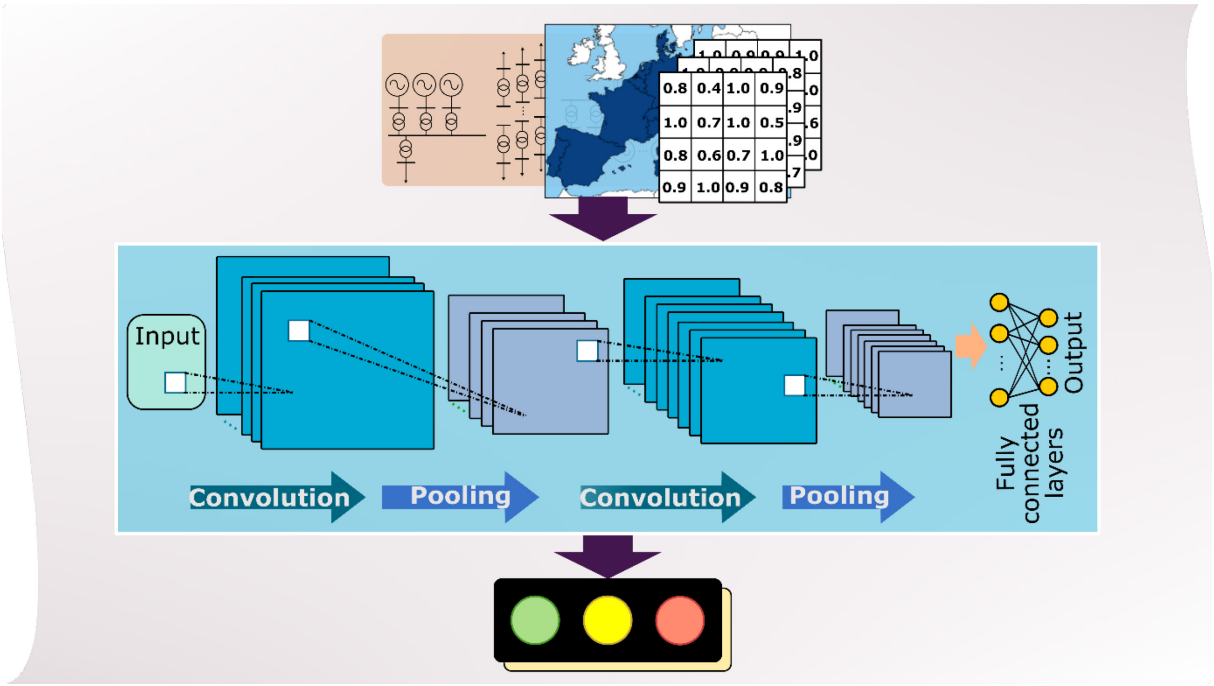

Source: © 11, 2024

Publisher:
Swiss Federal Office of Energy SFOE
Energy Research and Cleantech
CH-3003 Berne
www.energy-research.ch

Co-financing:
NA

Subsidy recipients:
Zurich University of Applied Sciences (ZHAW)
Gertrudstrasse 15, CH-8401 Winterthur
www.zhaw.ch

ETH Zürich – Research Center for Energy Networks (FEN)
Sonneggstrasse 28, 8006 Zürich
www.fen.ethz.ch

Authors:
Miguel, Ramirez-Gonzalez, ZHAW, ramg@zhaw.ch
Petr, Korba, ZHAW, korb@zhaw.ch
C. Yaman, Evrenosoglu, ETH Zürich, evrenosoglu@ethz.ch
Alexander, Fuchs, ETH Zürich, fuchs@fen.ethz.ch
Turhan, Demiray, ETH Zürich, demirayt@ethz.ch

SFOE project coordinators:
Dr. Michael Moser, michael.moser@bfe.admin.ch

SFOE contract number: SI/502660-01

Summary

The high proliferation of converter-interfaced generation at all voltage levels at the expense of fewer conventional plants at the transmission level will affect the traditional stability indicators defined by indices such as rate-of-change-of-frequency, frequency nadir, frequency recovery time. Transmission system operator's (TSO) need for a fast dynamic security assessor is imminent in such a habitat where the location and the amount and characteristics of electricity generation stochastically change daily and seasonally. The project is developing a fast AI/ML-based real-time dynamic security assessor (rtDSA) that can be deployed in the control room of a TSO as part of the SCADA/EMS. The primary role of the rtDSA will be to continuously scan grid's key performance indices (KPIs) and act as an "early warning system" for operators to take preventive actions proactively. The AI/ML-model will be developed using the ENTSO-E dynamic model, while appropriately considering the future scenarios for energy/infrastructure, and modelling resources connected at lower voltage levels. Swissgrid's involvement will ensure the developed solution satisfies practical requirements and is deployable, while Hitachi Energy will provide vendor insights for realistic assumptions on the measurement systems.

Within the current reporting period, the first set of input-output pairs that will be used for the ML-model are selected, along with the type of disturbances. The dynamic simulations are performed on the ENTSO-E initial dynamic model 2020, for a high-loading operating state, and the initial results are created for one type of outage (i.e., the outage of the largest generator at each country at a time). The initial set of outputs include the system ROCOF (for 500 ms and for 2'000 ms), the country ROCOF (for 500 ms and for 2'000 ms), the maximum standard deviation in the generator frequencies for each disturbance, the maximum deviation of the average country frequency from the average system frequency. The input-output pairs are stored in a tabular form in .csv file format. In addition, as part of the project tasks, two Convolutional Neural Network based approaches for the rapid detection of critical conditions in a given grid and the early assessment of its dynamic stability were investigated, and the obtained insights and results with the considered model architectures and application are provided.

Contents

List of figures

List of tables

List of abbreviations

AI	Artificial Intelligence
CE	Continental Europe
CF	Convolutional Filter
CIG	Converter-Interfaced Generation
CNN	Convolutional Neural Network
DER	Distributed Energy Resource
KPI	Key Performance Index
ML	Machine Learning
NA	Not Applicable
SEAM	Squeeze and Excitation Attention Mechanism
TSO	Transmission System Operator
TYNDP	Ten-year Network Development Plan
WAMS	Wide-Area Monitoring Systems
SFOE	Swiss Federal Office of Energy
WP	Work Package

1 Introduction

1.1 Context and motivation

The complexity of the analysis of large-scale power systems is increasing as converter-interfaced generation (CIG) technologies are adopted in combination with the electrification of e-mobility and heating demand. Due to the nature of the converters, the electromechanical dynamics followed by large disturbances are projected to be even faster. Therefore, analytically ensuring a stable grid operation, robust against large disturbances, is becoming an even more challenging task. Accurately modelling the impact of converter-interfaced resources on the grid stability problem and finding analytical solutions in a timeframe fast enough to implement real-time effective countermeasures is an arduous effort [1]-[4]. However, the wide-spread deployment of metering technologies such as GPS-synchronized time-stamped PMUs, available through wide-area monitoring systems (WAMS), and the advancements in deep learning techniques, present new opportunities to tackle this task from a data-driven perspective. Recent efforts, exploiting WAMS and advancements in data-driven approaches, demonstrate exciting potential and opportunities to effectively monitor and assess the dynamic stability of the grid in timeframes close to real-time [5], [6].

However, it is noted that the potentials of the data-driven methods are usually demonstrated in small-scale test examples and the focus has been primarily on the estimation of the condition of the system following a disturbance (i.e., to forecast whether the system is stable or not). In addition, the potential capabilities of data-driven approaches combined and strengthened with engineering know-how and experience (to identify countermeasures and improve system stability) have not been demonstrated.

Aiming to take a step forward, the proposed project will develop a tool for TSOs so that they are better equipped to securely accommodate new generation and demand without jeopardizing the robustness of the system as a whole. The proposed “early warning system” as a dynamic security assessor is going to be based on a machine-learning model [5]-[9]. The “early warning system” will continuously inform the operator whether the system is approaching critical stability boundaries and will provide predefined actions to keep the system “dynamically secure”, which implies that if a large disturbance happens the system can contain the frequency and voltage deviations in a reasonable timeframe. Essentially, the “dynamic security early warning system” will be based on the leverage and exploitation of the available data and will act as a traffic light for the operator. By helping TSOs to prepare for the emerging generation and demand habitat, the outcome of this project will support the successful implementation of the Swiss energy transition.

This is the first interim report of the earlyWARN project, where the related activities and results accomplished during the year 2024 are presented. In this regard, the report includes the documentation of tasks related to WP1 (Generation of the database and mapping of control actions) and WP2 (Development of the ML-based dynamic stability assessor).

1.2 Project objectives

The project proposes (i) to develop mechanisms to quickly assess relevant KPIs (e.g., voltage, angle, frequency), (ii) to identify the precarious states that can potentially lead to dynamic instabilities, and (iii) to recommend the most effective control actions to mitigate the potential stability problems. For this purpose, a fast real-time AI/ML-based dynamic security assessor will be designed for the TSO to identify the critical stability conditions early enough, which can, if no preventive action is taken, lead to large disturbances and cascaded events.

Furthermore, the framework and the process which will be used to create the ML-model will provide (i) insights to improve situational awareness, and (ii) a decision space to the operator by means of offline analysis.

The specific objectives of the project are described as follows:

1. Identify a set of operation conditions under different energy target scenarios covering different pathways towards 2050, where different load and generation combinations are observed, representing different grid operation states.
2. Identify different topologies considering (i) TYNDP actions, (ii) network configurations due to planned outages, and (iii) the location/type of critical disturbances.
3. Perform dynamic stability simulations on the detailed ENTSO-E model with sufficiently accurate representations of DERs in the distribution networks for each operational state, topology, and scenario, to create a sufficiently large training dataset for the ML model.
4. Identify the type of meaningful data to be used as the attributes to train the ML model.
5. Train and test the ML model using the deep learning method, based on convolutional neural networks (CNN), to design the “dynamic security assessor”, which will identify the critical stability conditions online and autonomously provide recommendation for control actions.
6. Assess the efficacy of the ML model in identifying precarious grid states and update the training data as required.

These objectives are aiming at answering the following questions:

- How can dynamic grid stability be assessed, and critical conditions be identified early on?
- And what are promising concepts for autonomous grid control?

2 Approach, method, results and discussion

The general structure of the work plan to accomplish the project objectives is illustrated in Figure 1.

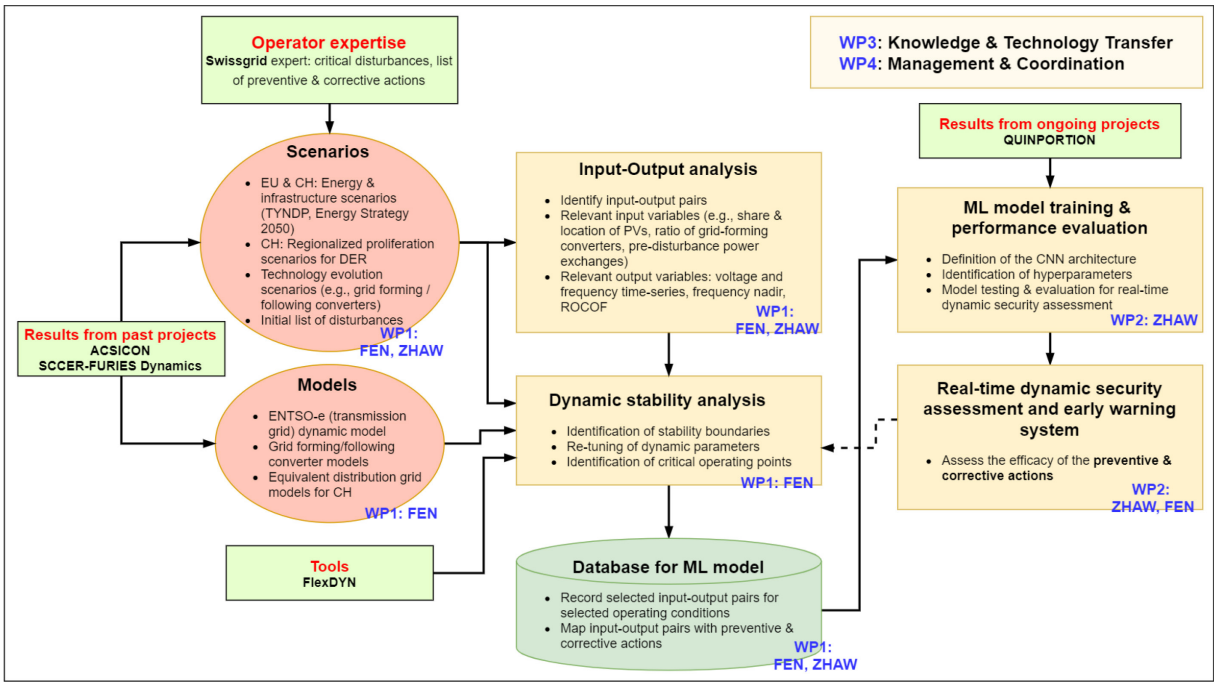

Figure 1: Overall framework and the work plan.

2.1 Generation of the database and mapping of control actions

As part of this work package, we have performed activities in four tasks:

T1. **Definition and creation of grid operation states for the ENTSO-E region to be simulated**: Two levels of loading conditions are selected: low and high, while two scenarios for PV and Wind generation are to be considered as low proliferation and high proliferation. It is noted that a feasible AC OPF solution is required for each combination of load-generation layout, which represents a power dispatch of the generating units, meaningful from AC perspective, with reasonable nodal voltages. Otherwise (i.e., with DC OPF solutions), a successful dynamic initialization (e.g., AVRs) of the generators is not achieved.

T2. **Definition/selection of relevant input and output information for dynamic security**: In addition to the input as described in T1 (i.e., loading level, share of converter-interfaced renewables such solar and wind), the selection of the disturbances which are meaningful and common and which have observable and sometimes drastic impacts on the stability metrics such as ROCOF, frequency nadir etc. are selected. The set of disturbances are as follows:

- Input i. The outage of the largest generator at each country
- Input ii. The outage of the highest-loaded cross-border transmission line (for each country pair)
- Input iii. The outage of the highest-capacity cross-border transmission line (for each country pair)
- Input iv. The loss of the largest load at each country

In addition to the input, the following list is the considered outputs (e.g., the results of the dynamic simulations):

- Output i. System ROCOF
- Output ii. Maximum deviation in the generator frequencies
- Output iii. Country ROCOF
- Output iv. Maximum deviation of the average country frequency from the average system frequency

T3. **Dynamic simulation of selected "operation states" and mapping of control actions**: Given the selected inputs in T2, time-domain simulations of the ENTSO-e dynamic model are performed in FlexDyn [10] to calculate the list of outputs identified in T2. FlexDyn is the in-house steady-state and dynamic analysis simulator designed for transmission and distribution systems. It was benchmarked against major commercial tools in previous projects such as ACSICON [11]. It is scalable and designed in a manner that the user can flexibly integrate new models such as converter-interfaced loads and generators thus allowing the user to easily modify and parameterize new components. The simulation engine is designed by using C++ while the whole simulation framework for bulk simulations can be designed using Python. The simulation framework is illustrated in Figure 2.

The ENTSO-E initial dynamic model, was published by ENTSO-E, converted from PowerFactory to the format of internal FEN tool, FlexDyn, tuned and benchmarked in SCCER-FURIES Dynamics and ACSICON projects. It contains 24'000 buses, 30'000 line elements (overhead, cable, transformer), 7'000 Loads and 5'000 static generators (impedance models), and 1'000 synchronous generators (dynamic 6th order machine model, Governor, AVR and PSS). The model snapshot represents a high-load case with a total load of about 458 GW in the ENTSO-E region.

Within the current reporting period, dynamic simulations are performed for the operation state corresponding to "generation and network layout in 2020, high loading level", for the outage of the maximum generating unit at each country.

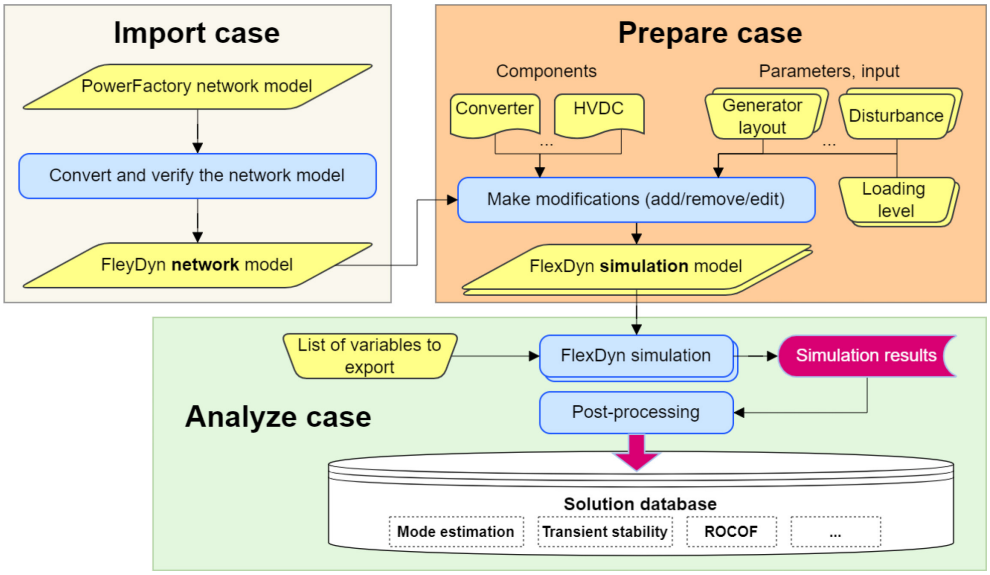

Figure 2: Simulation framework using FlexDyn

T4. **Creation of the solution database** (collection, arrangement, structuring of input-output pairs): The first version of the input-output list and the format for the solution database are agreed upon by ZHAW and FEN teams. The following input and output selections are stored in an .csv file and the .csv file is to be used in WP2 for training and testing a selected machine-learning algorithm.

Disturbances:

- Maximum generating unit at each country

System-level input:

- System loading level in the ENTSO-E region: **high load**.
- Share of wind/solar generation in the ENTSO-E region: **low wind/solar**.

System-level output:

- ROCOF (500 ms), $\bar{f}_{ENTSO-E}^{ROCOF500}$,calculated by using the first 500 ms of the average system frequency following a disturbance. Average system frequency is determined by averaging the generator frequencies in the ENTSO-E at each time instant following a disturbance. The results are presented in Figure 3. It can be observed that the outage of the largest generators in Belgium (BE), Bulgaria (BG), Netherlands (NL), Romania (RO) and Turkey (TR) leads to much larger deviations in frequencies resulting in relatively higher values for $\bar{f}_{ENTSO-E}^{ROCOF500}$.
- ROCOF (2000 ms), $\bar{f}_{ENTSO-E}^{ROCOF2000}$, calculated in a similar manner to $\bar{f}_{ENTSO-E}^{ROCOF500}$ but over a time inerval of 2'000 ms of the average system frequency following a disturbance.
- Maximum deviation in the generator frequencies, $\max\left[\sigma(f_{Generators})\right]$ determined by calculating the maximum of the standard deviations of generator frequencies, during the simulation period of 50 s following a disturbance. The results are presented in Figure 4. The results of the maximum deviations are highly correlated with those presented for ROCOF in Figure 3. It is important to note that the impact of an outage depends highly on the location of the generator as well (in addition to its size).

Country-level output:

- ROCOF (500 ms) per country, $\bar{f}_{Country}^{ROCOF500}$, calculated by using the first 500 ms of the average country frequency. Average country frequency is determined by averaging the frequency of

each generator in the respective country at each time instant following a disturbance. The results are presented in Figure 5 and in Table 1. As expected, the impact of the outage of the maximum power generating unit in a given county is mostly the highest in the country of the disturbance. This result can be observed easily, for example, for Spain, Switzerland, Netherland, Romania and Turkey, in Figure 5, and by observing the colour of the diagonal elements in Table 1. The colouring is performed per row (i.e., per the outage location of the largest generating unit). That means, the largest value in a given row is denoted by **red** and as the values in that row are smaller than the largest value, they are assigned tones of red and tones of blue, while smallest value is dark **blue**. For example, the outage in Belgium (BE) results in largest country ROCOF deviation in Belgium by 39 mHz/s, and it is the diagonal entry, denoted by red. The same outage results in a ROCOF deviation of 23 mHz/s in NL, denoted by light red, while those unaffected countries are denoted by blue.

- ROCOF (2000 ms) per country, $\bar{f}_{Country}^{ROCOF2000}$, calculated calculated in a similar manner to $\bar{f}_{Country}^{ROCOF500}$ but over a time interval of 2'000 ms of the average country frequency. Average country frequency is determined by averaging the frequency of each generator in the respective country at each time instant following a disturbance.
- Maximum deviation of the average country frequency, $\bar{f}_{Country}$, from the average system frequency, $\bar{f}_{ENTSO-E}$,following a disturbance, during the simulation period of 50 s. The results are presented in Figure 6.

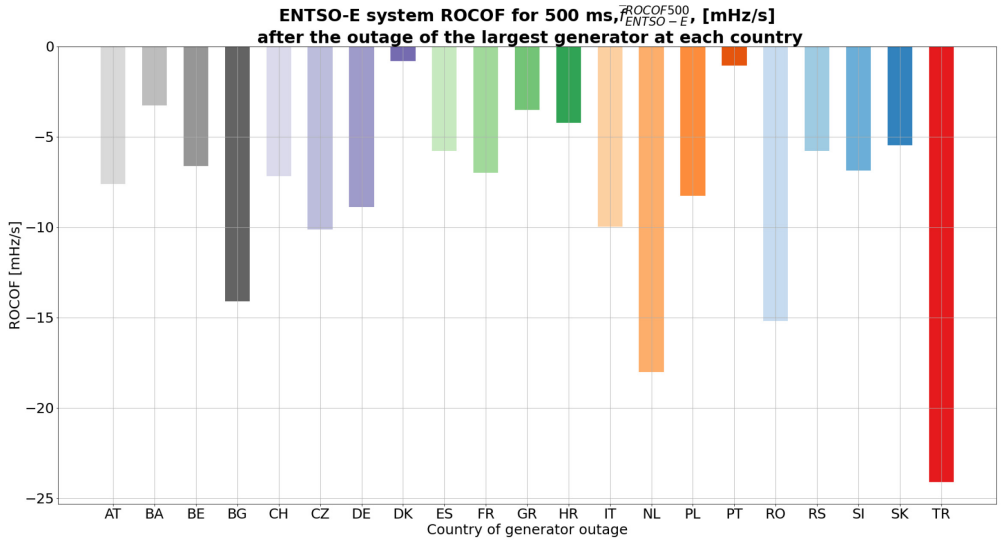

Figure 3. The system ROCOF for 500 ms, following the outage of the largest generator in each country at a time.

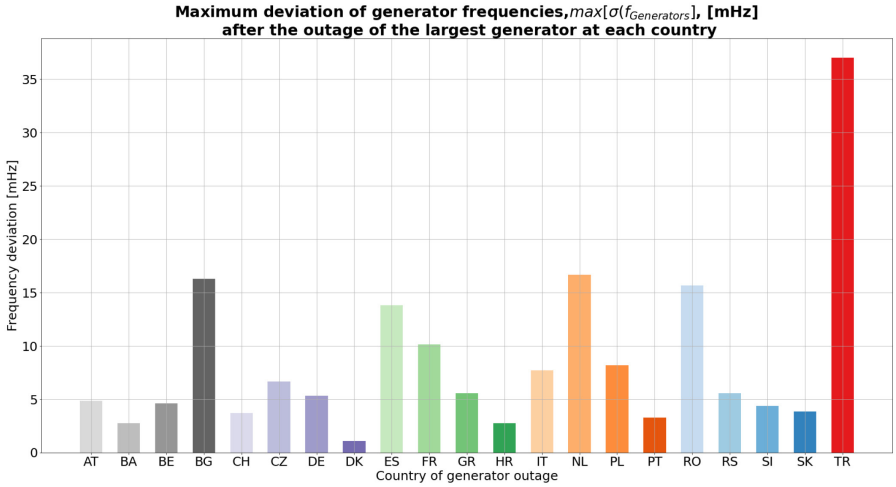

Figure 4: The maximum deviation of generator frequencies following the outage of the largest generator in each country at a time.

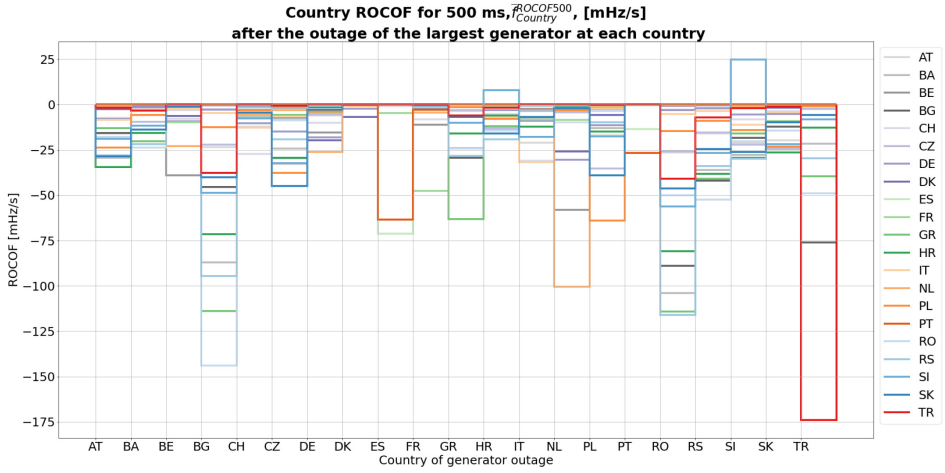

Figure 5: The country ROCOFs for 500 ms following the outage of the largest generator in each country at a time.

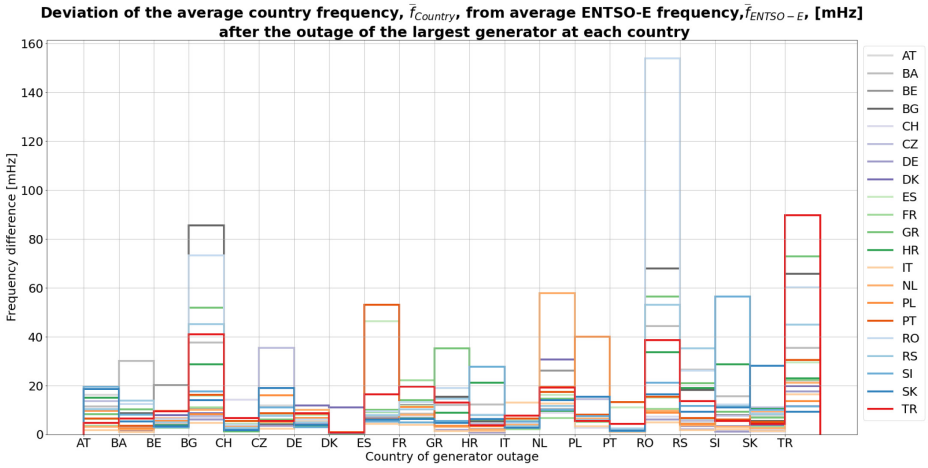

Figure 6: Deviation of the average county frequency from the average ENTSO-E frequency, calculated for all countries following the outage of the largest generator in each country at a time.

Table 1: The country ROCOFs for 500 ms following the outage of the largest generator in each country at a time. The colouring is performed per row (i.e., per the outage location of the largest generating unit). That means, the largest value in a given row is denoted by **red** and as the values in that row are smaller than the largest value, they are assigned tones of red and tones of blue, while smallest value is dark **blue**. For example, the outage in Belgium (BE) results in largest country ROCOF deviation in Belgium by 39 mHz/s, and it is the diagonal entry, denoted by red. The same outage results in a ROCOF deviation of 23 mHz/s in NL, denoted by light red, while those unaffected countries are denoted by blue.

Country of generator outage	Country ROCOF for 500 ms, [mHz/s] after the outage of the largest generator at each country																				
	AT	BA	BE	BG	CH	CZ	DE	DK	ES	FR	GR	HR	IT	NL	PL	PT	RO	RS	SI	SK	TR
AT	16	30	1	16	8	29	8	3	0	1	13	34	8	1	24	0	18	28	19	29	2
BA	10	1	0	20	2	9	2	0	0	0	20	16	3	0	6	0	24	22	12	14	3
BE	3	0	39	0	8	2	9	6	0	10	0	1	2	23	1	0	0	0	1	1	0
BG	23	87	0	46	3	22	3	1	0	0	114	71	5	0	12	0	144	95	49	40	38
CH	12	3	6	0	27	7	10	5	0	6	0	5	13	6	3	0	0	2	8	5	0
CZ	33	24	2	8	9	30	15	7	0	1	6	29	7	3	38	0	9	19	32	45	1
DE	6	1	15	0	10	6	18	20	0	4	0	2	3	26	4	0	0	1	3	3	0
DK	0	0	0	0	0	0	2	7	0	0	0	0	0	1	0	0	0	0	0	0	0
ES	0	0	0	0	1	0	0	0	71	5	0	0	0	0	0	64	0	0	0	0	0
FR	2	0	11	0	8	1	2	1	3	48	0	0	3	4	0	3	0	0	1	0	0
GR	4	24	0	29	0	3	0	0	0	0	63	16	1	0	2	0	24	28	10	7	6
HR	13	14	0	13	5	13	3	1	0	1	12	6	7	1	8	0	14	19	8	16	2
IT	21	7	4	1	31	8	9	3	0	8	1	12	32	3	3	0	1	4	18	7	0
NL	5	1	58	0	10	4	31	26	0	9	0	1	2	101	3	0	0	0	2	2	0
PL	17	13	1	4	3	35	11	6	0	0	2	15	2	2	64	0	4	10	18	39	0
PT	0	0	0	0	0	0	0	0	14	0	0	0	0	0	0	27	0	0	0	0	0
RO	26	104	0	89	3	26	3	1	0	0	114	81	5	0	15	0	50	116	56	46	41
RS	16	36	0	42	2	15	2	1	0	0	41	38	4	0	9	0	52	34	27	25	7
SI	21	28	1	18	8	22	6	1	0	1	16	29	11	1	14	0	20	30	25	26	2
SK	20	23	0	12	4	25	5	2	0	0	9	26	4	1	23	0	14	22	22	10	1
TR	3	22	0	76	0	2	0	0	0	0	40	13	0	0	1	0	49	30	8	6	174

2.2 Development of the ML-based dynamic stability assessor

Since CNNs are a class of advanced ML algorithms that have proven to be very successful in the development of data-driven solutions for high-complexity problems in different fields [6], [12], the use of them has been considered in this project as the core component of the “dynamic stability assessor”. Conceptually, a CNN can be described through the basic architecture Figure 7 [7]. It consists of multiple layers of interspersed convolution and pooling operations, followed by one or two fully connected (dense) layers to combine the information from preceding operations and map it into a class probability distribution.

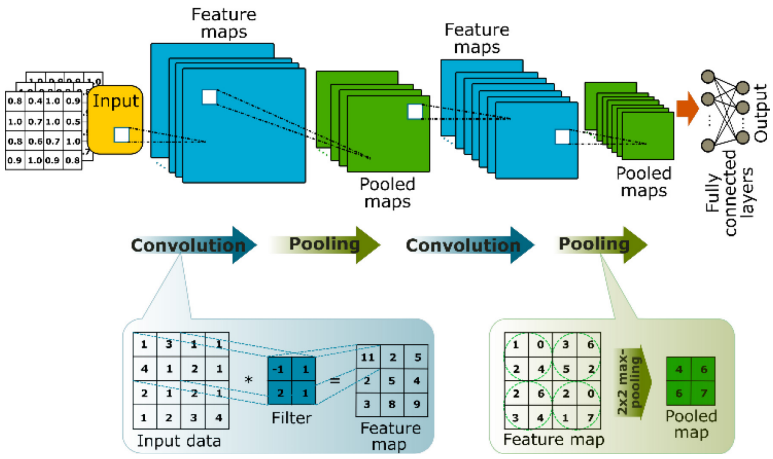

Figure 7: Basic architecture of CNNs.

Naturally, the main building block of CNNs is the convolution operation, which through a number of filters with a certain kernel size can extract important features and identify complex patterns from the given input. On the other side, pooling operation are included to progressively manage and reduce the spatial dimensions of data and focus on the most significant features by determining for instance the maximum or average value within different regions of the provided input maps. After these operations, obtained multidimensional arrays are converted into one dimensional vector before being supplied to the fully connected layers. In practice, some other computations such as batch normalization and dropout are additionally integrated into the structure to facilitate the learning task and improve model performance [13].

In general, the architecture in Figure 7 contains a number of trainable parameters associated with the weights of the convolutional filters and the fully connected layers. Based on the backpropagation algorithm [14], these parameters can be iteratively adjusted during the training phase to minimize a given loss function $F(\cdot)$ and calculate a set of values that provide a certain predicting performance. The updating process is represented in equation (1), where α is a given network parameter, ∇ denotes the gradient, η is the learning rate, and k refers to the training instant.

$$\alpha_k = \alpha_{k-1} - \eta \nabla_\alpha \mathcal{F}(\alpha_t) \tag{1}$$

To be able to use a CNN for the application contemplated in this project, a number of decisions related for example to the configuration and arrangement of components such as convolution, pooling, and fully connected layers, as well as involved activation functions, have to be made. Additionally, the proper incorporation of operations such as batch normalization and dropout to improve training convergence speed and model generalization ability has to be carried out. In this way, with an initial arrangement, the number of convolutional filters, kernel sizes for convolution/pooling, dropout rate, and nodes of dense layers must be specified. Then, hyperparameters concerning how the network will be trained (such as batch size, epochs, loss function, and the optimizer) are to be denoted. Important to highlight here is that, in general, the building of a successful CNN model involves an iterative process where initial hyperparameters associated with both network structure and learning algorithm may be adjusted until the model is able to acceptably deal with the given problem.

Now, in order to get some insights about the rapid detection of critical conditions in a given grid, the early assessment of the dynamic stability, as well as the required architecture of a CNN for such application, two approaches for transient stability prediction were investigated here with the simulation model of a relatively small power system, as described next.

2.2.1 Use of time-series based inputs after a large disturbance

This approach is based on the use of post-disturbance measurements after the occurrence of a perturbation event such as a three-phase fault on a transmission line. In this way, time series of bus voltage magnitudes and phase angles are assembled into a two-channel arrangement to shape the input examples for a CNN, which consider recordings (with a given sampling time) from the moment the disturbance occurs until a predefined time instant (260 ms in this study).

In order to build a sample dataset for model training purposes, new steady state operating conditions were produced from a base case scenario by varying both the system load and generation of the test power grid. Then, by performing time domain simulations, a three-phase fault was applied at 0% and 25% of the length of each transmission line for each of these operational points. The fault was then removed by tripping the involved line after 300 ms. A total simulation time of 5 s was considered in each particular case to determine if the system becomes unstable after the contingency. Based on this, a representative set of input and output observations consisting of time series of voltage magnitudes and phase angles at every bus on one side, and transient angle stability condition in terms of “stable” or “unstable” on the other side, was collected. An illustration of the involved information in this sense is provided in Figure 8 for a case where the system response is stable.

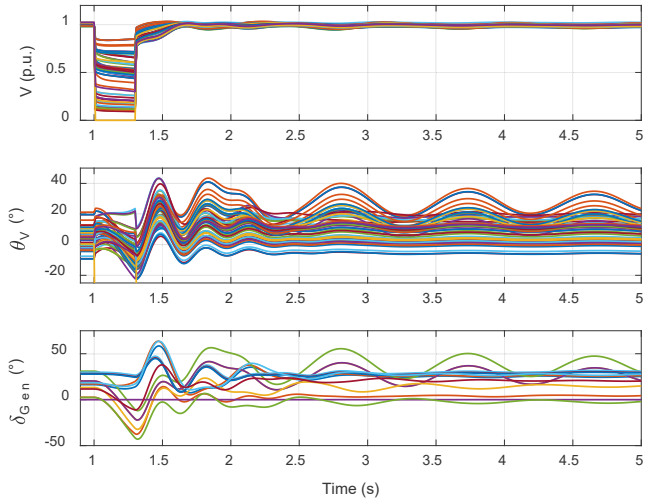

Figure 8. Information from a given stable case.

By taking into account the trajectory of the power angle of the machines after the disturbance, the transient stability of the system is assessed in the following way [15]:

$$\eta = \frac{360-\delta_{\max}}{360+\delta_{\max}} \text{x}100 \tag{1}$$

$$\text{System status} = \begin{cases} Stable & \text{if} \quad \eta > 0 \\ Unstable & \text{Otherwise} \end{cases} \tag{2}$$

where η is the transient stability index and δ_{max} refers to the maximum angle separation between two generators of the system after the contingency. According to this, a set of 756 input-output pairs were selected to be used in the design of the CNN for the assumed classification task.

The particular CNN structure considered here is illustrated in Figure 9, which includes two convolutional layers (CLs) linked to activation functions of the ReLU type [14], batch normalization operations, a Squeeze and Excitation attention mechanism (SEAM) [16], [17], a dropout regularization block with a dropout of 0.25, a flattening layer, and one dense layer with two units connected to Softmax activation functions. The number of convolutional filters (CFs) for the first and second CL was set to 64 and 32,

respectively, with a kernel size of 2x2 for both of them. The SEAM was incorporated into the network as a mean to enable the model to automatically learn the importance of a given set of features maps, and focus on the most relevant features by reweighting these maps through the channel attention mechanism. The second dense layer of the SEAM was configured with 32 units to match the number of CFs used in the second CL of the network.

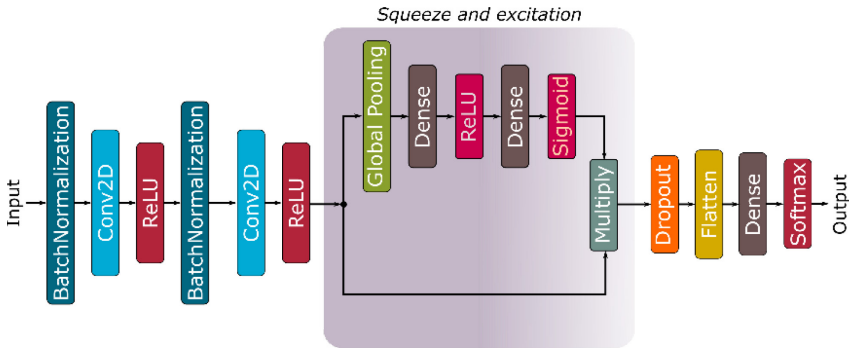

Figure 9: CNN model structure with SEAM.

To be able to use the collected information in the training of the model in Figure 9, a rescaling process was first applied to the input examples to transform their values into the range 0-1. On the other side, the categorical outputs ("Stable" and "Unstable") were turned into numerical information through one hot encoding, creating a matrix of binary data with a 1 on the respective column to mark a given category and 0 otherwise. Due to the class imbalance in the sample dataset, where the "Stable" class is dominant, a stratified *k*-fold cross-validation technique was adopted to ensure the fair representation of each class in the training and evaluation of the model, avoid biased predictions, and achieve more reliable estimates of overall model performance [13]. Regarding the definition of learning process, a categorical crossentropy loss function and the Adam optimizer were applied in the configuration, and the number of training epochs was set to 300. Furthermore, to get an accurate indication of the performance of the proposed machine learning model on the sample dataset, five repetitions of the *k*-fold cross-validation procedure (with *k*=3) were carried out here. In this way, the achieved mean results during the training phase (across all folds and over the assumed five repetitions) are illustrated in Figure 10 and Figure 11, which respectively show the obtained accuracy and loss learning curves. The difference in the training performance with and without the SEAM are emphasized in Figure 10 by smoothed representations from polynomial approximations (indicated by the green and red curves, respectively).

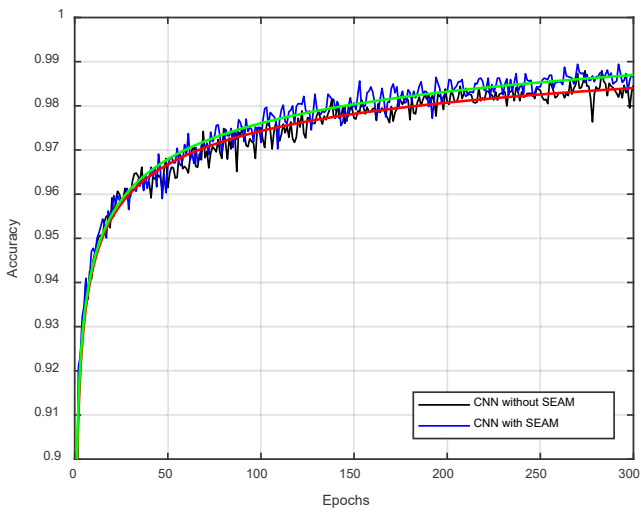

Figure 10: Accuracy curves during model training.

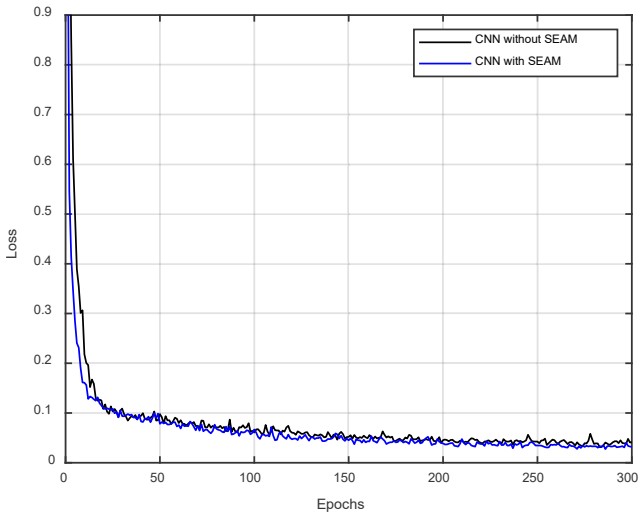

Figure 11: Loss curves during model training.

As highlighted in Figure 10, the inclusion of the SEAM can provide a slightly improved learning performance from a comparatively better convergence rate and model accuracy. In terms of the evolution of the training loss, Figure 11 shows that it decreases to start settling in a minimum point, with lower values provided in general by the CNN model that incorporates the considered attention mechanism. The prediction response of the involved CNN models can be quantified in terms of the Accuracy, Precision, Recall, and F1-Score metrics [12] across all folds held out as test sets and over all repeats. In doing so, the mean performance given in Table 2 was determined. As it can be observed, the CNN model with the SEAM was able to achieve superior mean score values and slightly low standard deviations (Std), as compared to the structure with no SEAM, showing a relatively better model prediction and a more reliable behavior to unseen data.

Table 2: Model performance metrics.

Model	**Metric (%)** Mean/Std. values			
	Accuracy	**Precision**	**Recall**	**F1-score**
SEAM-CNN	**97.746**	**97.652**	**97.653**	**97.652**
	0.967	1.035	1.035	1.035
CNN	97.447	97.387	97.381	97.387
	1.069	1.076	1.078	1.076

2.2.1 Use of steady-state inputs under normal operating conditions

Approaches relying completely on the use of post-disturbance dynamics to correctly evaluate a given condition necessarily require the existence of system incidents. However, instead of reacting to a critical event when it has already happened, the idea investigated in this section is the adoption of a proactive tactic for the anticipation and prevention of a potential problem based only on steady-state information (under normal operating conditions).

A new dataset was generated in this case with a new collection of representative samples for system stable and unstable conditions. A three-phase fault at each transmission line under a wide range of loading operating conditions was also assumed. On this occasion, the fault is released by tripping the corresponding line after 150 ms. Moreover, the pre-fault active and reactive power through every transmission line in the system, the voltage magnitudes at the terminal buses of the involved lines, as well as an indication of the line where the fault is applied, were gathered as model input examples here. On the other part, for the target output, the associated transient stability condition of the grid was determined from dynamic simulations using again the expressions (1) and (2) above. According to this, a total of 5040 input-output observations were collected for training purposes. Examples of related stable and unstable situations after the applied event are one more time illustrated in Figure 12.

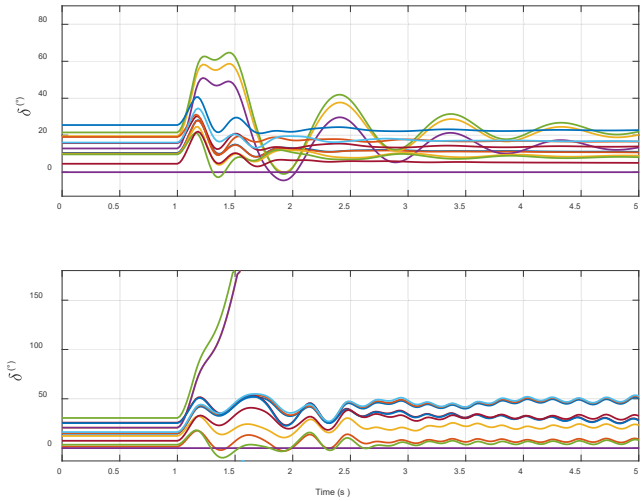

Figure 12: Example of stable (upper plot) and unstable (lower plot) cases.

The considered CNN model this time is shown in Figure 13, where four sets of convolutional layers and two fully connected layers were considered along with batch normalization, max pooling, dropout, and flatten operations (arranged as indicated). The Conv2D blocks were configured with 256, 128, 64, and 32 filters, respectively, where the kernel size was set to 1x3 in all of them. Besides, ReLU type activation functions were also associated with each of these elements. The included max pooling layer was defined with a pool size and a stride of 1x3, and the rate attribute of the dropout operation was set to 30%. On the other hand, the dense layers were specified with 100 and 2 units, and ReLU and Softmax activation functions, respectively.

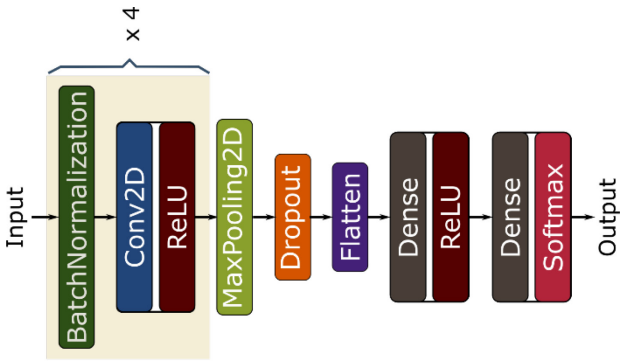

Figure 13: Considered CNN model.

A layer freezing mechanism was incorporated into the model of Figure 13 so that the trainable parameters of the four series of components involving convolution operations were temporarily “frozen” after a certain epoch during the learning process. For this purpose, the loss function value was monitored at

the end of every training epoch. Therefore, the aforementioned parameters were not updated anymore after detecting that the considered measure was no longer decreasing with respect to a reference value. After that, the training continued for the rest of trainable parameters in the network, but the ones belonging to the indicated elements remained fixed.

For training, performance estimation, and model selection, a *k*-fold cross-validation approach (with *k*=3) was also followed here. In order to ensure the same percentage of samples for each class in every fold, a stratified variation was once again applied. This *k*-fold cross-validation process was repeated five times with the number of training epochs set to 200 in this case, the loss function specified as categorical crossentropy class, and the optimizer set to the Adam algorithm. The average performance of the proposed model during the training phase, with and without layer freezing, is shown in Figure 14 and Figure 15 in terms of accuracy and minimization of the loss function.

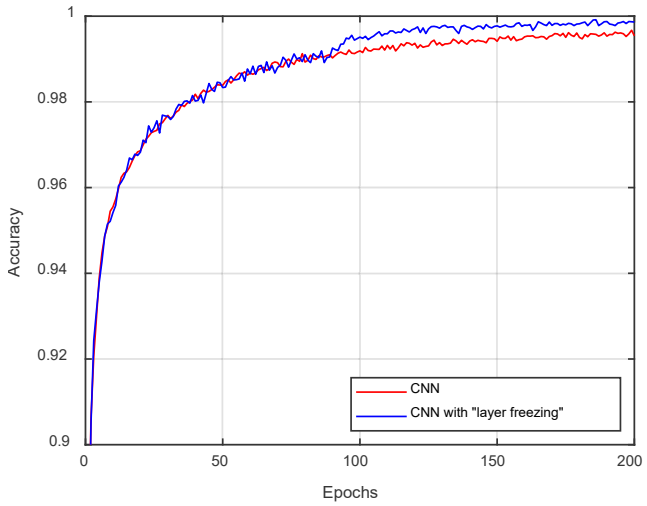

Figure 14: Average accuracy.

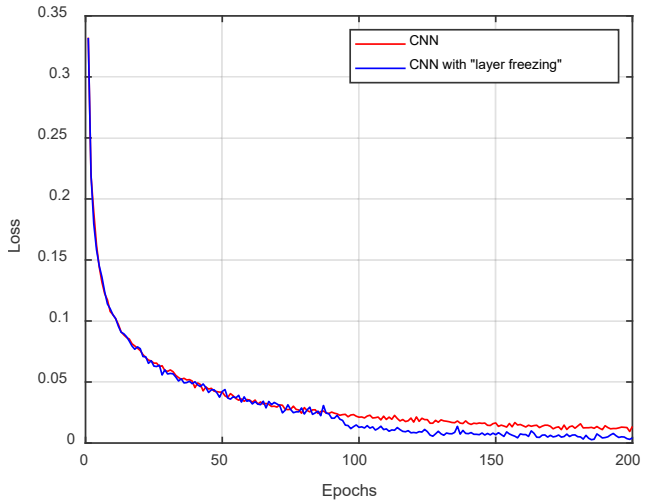

Figure 15: Average loss.

As observed from these two previous figures, it is evident that the model with the layer freezing alternative is able to achieve higher accuracy performance and lower loss values, as compared to the model where the whole set of trainable parameters is continuously updated over the total number of predefined training epochs. Besides, it can be implied from these results that the capability of the front layers in extracting general features has been reached in less than 90 epochs. However, for deeper layers such as the two dense ones included in the model here, it seems that the longer training allows the fine-tuning of these layers to better extract more task-specific features. Regarding computational time, the "layer freezing" arrangement here allowed the reduction of the learning time by around 20%, which becomes of great relevance when training very large models.

By using all data folds set aside for testing purposes over the five assumed repetitions, the performance of the approach is quantified though the average metrics in Table 3, which confirm the enhanced prediction capability of the CNN with layer freezing strategy as compared to a corresponding base model.

Table 3: Model performance metrics (test set).

Model	**Metric (%)** Mean/Std. values			
	Accuracy	**Precision**	**Recall**	**F1-score**
CNN-Layer freezing	**98.041**	**98.040**	**98.038**	**98.040**
	0.261	0.259	0.261	0.259
CNN	97.765	97.762	97.761	97.762
	0.260	0.262	0.263	0.262

3 Conclusions and outlook

Motivated by global factors such as decarbonization, decentralization, and digitalization, power systems are experiencing an unprecedented transformation, rendering the operation and control of transmission and distribution grids more complex, while being exposed to more uncertainty. Consequently, the capabilities of traditional analytical approaches are being surpassed under such evolving scenarios, and transmission system operators are faced with an unprecedented number of operational challenges and decisions to appropriately identify system vulnerabilities online and quick enough to efficiently respond to a potential unstable situation.

In this sense, with the idea of developing a fast AI/ML-based real-time dynamic security assessor (rtDSA) to support the stable operation of the CE power grid, the earlyWARN project's tasks related to the generation of a database (for model training purposes), and the assembly of the rtDSA itself, are reported. In this context, the progress and results during the year of 2024 for specific activities such as creating grid operation states, definition/selection of relevant input and output information, dynamic simulation of selected "operation states," and creation of the solution database are described. Moreover, different insights on the fast online stability assessment of power system dynamics have also been gained through the exploration of two CNN based approaches to predict the transient stability of a sample power system. On one side, post-disturbance time series of bus voltage magnitudes and phase angles are considered to train and evaluate the performance of a CNN with an attention mechanism, where the output of the network is intended to categorize the status of the system in terms of "stable" or "unstable." On the other side, steady-state variables were used as inputs to another CNN architecture where a freezing strategy was applied to the trainable parameters of some selected front layers of the model. Target outputs are also defined according to the same previous categories (as related to the transient stability of the system). By using a test set from the collected input-output observations in each case, trained CNN models show their potential ability to quickly predict if the system will evolve to an unstable state after the considered disturbance occurred in the first approach or, in the second studied

alternative, if the grid in normal operating conditions could move towards such a state in the event that this perturbation actually happens.

The following steps of the project can be listed as follows:

1. The methodology developed in WP2 will be applied to the current results in WP1, and the efficiency of using the selected outputs (provided in the form of .csv file containing the scalar stability indicators) will be assessed. Accordingly, new outputs will be added to the output list and training and testing of the ML model will be repeated. The ML-model will be trained and tuned so that the correlations presented in Table 1 can be potentially identified. For example, it is expected and observed in Table 1 that the outage of the maximum generator in Portugal results in the highest ROCOFs in Portugal and Spain, respectively (corresponding values in red), while the impact of an outage of the maximum generator in Bosnia is more distributed, affecting the ROCOFs in Bulgaria, Greece, Croatia, Romania, Serbia, Slovenia and Slovakia.
2. The dynamic simulations of the outage of the highest-loaded cross-border transmission line (for each country pair) will be performed for the same input (i.e., loading level and generation layout) and added to the solution database.
3. The dynamic simulations of the outage of the highest capacity cross-border transmission line (for each country pair) will be performed for the same input (i.e., loading level and generation layout) and added to the solution database.
4. The dynamic simulations of the loss of the largest load at each country will be performed for the same input (i.e., loading level and generation layout) and added to the solution database.
5. The loading level and generation layout will be updated so that a meaningful AC solution is obtained, in coordination with Swissgrid.
6. Further investigations will also be performed to scale the results of the explored CNN models for very large power system applications, including further exploitation and enhancement of their capabilities.

4 Publications and other communications

[A] M. Ramirez-Gonzalez, F. R. Segundo Sevilla, P. Korba, R. Castellanos, “CNN with squeeze and excitation attention module for power system transient stability assessment,” 12th International Conference on Smart Grid, Setubal, Portugal, May 27-29, 2024.

[B] M. Ramirez-Gonzalez, F. R. Segundo Sevilla, P. Korba, “Power system transient stability prediction with a CNN trained with steady-state input variables,” 8th International Conference on Power and Energy Engineering, Chengdu, China, Dec. 20-22, 2024 (Submitted / Under review).

5 References

[1] ENTSO-E, SPD DSA Task Force Dynamic Security Assessment (DSA), RG-CE System Protection & Dynamics Subgroup, April 2017

[2] M. Paolone et al., Fundamentals of power systems modelling in the presence of converter-interfaced generation, Electric Power Systems Research, vol. 189, Dec. 2020.

[3] F. Milano, F. Dörfler, G. Hug, D. J. Hill and G. Verbič, "Foundations and Challenges of Low-Inertia Systems (Invited Paper)," 2018 Power Systems Computation Conference (PSCC), Dublin, Ireland, 2018.

[4] D. Ramasubramanian, Z. Yu, R. Ayyanar, V. Vittal and J. Undrill, "Converter Model for Representing Converter Interfaced Generation in Large Scale Grid Simulations," in IEEE Transactions on Power Sys-tems, vol. 32, no. 1, pp. 765-773, Jan. 2017.

[5] R. Segundo, Y. Liu, E. Barocio, P. Korba, et. al., Application of spatio-temporal data-driven and machine learning algorithms for security assessment, IEEE Technical Report (TR104), 2022.

[6] M. Nazaris, S. Asadi, N. Mohammadi, et. al., Application of Machine Learning and Deep Learning Methods to Power System Problems, Cham: Springer, 2022.

[7] M. Ramirez-Gonzalez, F. R. Segundo Sevilla, P. Korba, and R. Castellanos, “Convolutional neural nets with hyperparameter optimization and feature importance for power system static security assessment,” Electric Power Systems Research, vol. 211, June 2022.

[8] M. Ramirez-Gonzalez, L. Nösberger, F. R. Segundo Sevilla, P. Korba, “Small-signal stability assessment with transfer learning-based convolutional neural networks,” IEEE Canada Electrical Power and Energy Conference (EPEC 2022), Victoria, Canada, Dec. 5-7, 2022.

[9] M. Ramirez-Gonzalez, F. R. Segundo Sevilla, P. Korba, “Power System Inertia Estimation Using a Residual Neural Network Based Approach,” 4th Global Power, Energy and Communication Conference (GPECOM2022), Cappadocia, Turkey, June 14-17, 2022.

[10] T. Demiray, “FlexDyn: An RMS-based dynamic stability analysis tool for very-large interconnected electric transmission systems”, 2017, fen/flexdyn .

[11] “ACSICON: Novel Analysis and Control Solutions for Dynamic Security Issues in the Future”, Swiss Federal Office of Energy, Final Report SI/501728, 2021.

[12] P. Fergus, C. Chalmers, Applied Deep Learning: Tools, Techniques, and Implementation, Cham: Springer, 2022.

[13] J. Brownlee, Better Deep Learning: Train Faster, Reduce Overfitting, and Make Better Predictions. Machine Learning Mastery, v1.3, 2019.

[14] C. Aggarwal, Neural Networks and Deep Learning. Cham: Springer, 2018.

[15] P. Kundur, O. Malik, Power System Stability and Control. New York: McGraw-Hill, 2022.

[16] J. Hu, L. Shen, S. Albanie, et al., “Squeeze-and-Excitation Networks,” IEEE Trans. on Pattern Analysis and Machine Intelligence, 42:8, pp. 2011-2023, Oct. 2020.

[17] X. Jin, Y. Xie, X-S. Wei, et al., “Delving deep into spatial pooling for squeeze-and-excitation networks,” Pattern Recognition, 121, pp. 1-12, 2022.